

INTEGRAL observations of PSR J1811–1925 and its associated Pulsar Wind Nebula

A.J. Dean,¹ A. De Rosa,² V.A. McBride,¹ R. Landi,³ A.B. Hill,¹ L. Bassani,³
A. Bazzano,² A.J. Bird,¹ P. Ubertini,²

¹*School of Physics and Astronomy, University of Southampton, Highfield, SO17 1BJ, United Kingdom*

²*INAF/IASF, via del Fosso del Cavaliere 100, Roma, 00113, Italy*

³*INAF/IASF, via P. Gobetti 101, Bologna, 40129, Italy*

17 August 2021

ABSTRACT

We present spectral measurements made in the soft (20–100 keV) gamma-ray band of the region containing the composite supernova remnant G11.2-0.3 and its associated pulsar PSR J1811–1925. Analysis of INTEGRAL/IBIS data allows characterisation of the system above 10 keV. The IBIS spectrum is best fitted by a power law having photon index $\Gamma = 1.8^{+0.4}_{-0.3}$ and a 20–100 keV flux of 1.5×10^{-11} erg cm⁻² s⁻¹. Analysis of archival *Chandra* data over different energy bands rules out the supernova shell as the site of the soft gamma-ray emission while broad band (1–200 keV) spectral analysis strongly indicates that the INTEGRAL/IBIS photons originate in the central zone of the system which contains both the pulsar and its nebula. The composite X-ray and soft gamma-ray spectrum indicates that the pulsar provides around half of the emission seen in the soft gamma-ray domain; its spectrum is hard with no sign of a cut off up to at least 80 keV. The other half of the emission above 10 keV comes from the PWN; with a $\Gamma=1.7$ its spectrum is softer than that of the pulsar. From the IBIS/ISGRI mosaics we are able to derive 2σ upper limits for the 20–100 keV flux from the location of the nearby TeV source HESS J1809–193 to be 4.8×10^{-12} erg cm⁻² s⁻¹. We have also examined the likelihood of an association between PSR J1811–1925 and HESS J1809–193. Although PSR J1811–1925 is the most energetic pulsar in the region, the only one detected above 10 keV and thus a possible source of energy to fuel the TeV fluxes, there is no morphological evidence to support this pairing, making it an unlikely counterpart.

Key words: Stars: pulsars: individual: PSR J1811–1925 – Stars: supernovae: individual: G11.2-0.3 – Gamma-rays: observations

1 INTRODUCTION

Recently, *Chandra* and *XMM-Newton* X-ray observations have allowed detailed morphological studies of Pulsar Wind Nebulae (PWN), resolving complex structures within the general envelope of the plerion, including toroidal features, axial jets and wisps on arc second angular scales; for recent reviews see Kaspi et al. (2006) and Gaensler & Slane (2006). The PWN are generally associated with young energetic pulsars with ages of less than a few tens of thousands of years such as the cases of the Crab and Vela systems (Weisskopf et al. 2004, Kirsch et al. 2006; Helfand et al 2001; Pavlov et al. 2003; Mangano et al. 2005). It is generally thought that the radiation mechanism from radio to X-ray wavelengths is due to synchrotron emission as a result of electrons injected by the pulsar, with the radio emission due to the relic electrons and X-rays resulting from freshly injected electrons. The diminishing angular sizes of the spectral images with increasing photon energy provide strong evidence for synchrotron cooling in a number of cases. However the *Chandra* spectral images show that the separate mor-

phological regions within the overall nebular configuration, such as a jet, counter jet, torus, extended PWN, moving hot spots and so on are characterised by distinct spectral indices in the X-ray domain. This indicates that the transport of the energetic electrons is not simply “isotropically outwards” from a central source, but can be the result of collimated beams, sometimes containing moving blobs with considerably harder spectra than the surrounding emission structures (e.g. Mori et al. 2004 for the case of the Crab nebula).

The study of these objects in the soft gamma-ray domain, adjacent to the X-ray band, can provide key information to disentangle the mechanisms active in different emitting regions. In view of this, the IBIS gamma-ray imager on board INTEGRAL is a powerful tool for the study of PWN systems, allowing source detection above 20 keV with sensitivity of the order of mCrab. Moreover, the recent survey performed with the HESS (High Energy Stereoscopic System) telescope array revealed the existence of emission at TeV energies from the vicinity of a number of pulsar wind nebulae (Aha-

ronian et al. 2006; 2007). The combined analysis of X-/gamma-ray and Very High Energy (VHE) emission is of key importance to estimate the relative contribution of synchrotron and inverse Compton mechanisms and thus to derive information on the magnetic field of the nebula and the spatial energy distribution of the accelerated particles.

2 PSR J1811–1925

An interesting case to investigate is the 65 ms pulsar PSR J1811–1925, discovered in X-rays by *ASCA* in the supernova remnant (SNR) G11.2-0.3 (Torii et al. 1997). It is a composite SNR showing both an extended shell component and a compact plerionic component. This discovery strongly suggests a direct association of the pulsar with the SNR and with a “guest star” witnessed by Chinese astronomers in A.D. 386 as proposed by Clark & Stephenson (1977). The distance of the system is ~ 5 kpc as inferred from H I measurements (Becker, Markert & Donahue 1985; Green et al. 1988). Thanks to X-ray observations performed by *Chandra* (Kaspi et al. 2001) it was possible to localise the pulsar to within a few arc seconds from the geometric centre of the shell of the SNR (Tam & Roberts 2003), thus providing an indication that the system may be young.

A more detailed analysis of the *Chandra* data combined with VLA observations (Roberts et al. 2003) demonstrates the separation of the PWN from the surrounding shell, suggesting that the reverse shock has not yet reached the PWN, thus implying the system age is no more than ~ 2000 yr. The youth of the system was also confirmed using VLA data to measure the expansion of G11.2-0.3 over a period of 17 yr, which provides a direct age estimate in the range 960–3400 yr, which is compatible with the ~ 1620 yr age derived on the basis of the direct association with the supernova event of A.D. 386 (Tam & Roberts 2003). However, if it is assumed that the energy loss from the pulsar is a result of magnetic dipole radiation losses, with a braking index of $n \sim 3$, the spin down age of the pulsar, $P/2\dot{P}$, would imply that the supernova explosion took place around 24000 years ago. This apparent age discrepancy can be explained by assuming that the initial spin period of the pulsar was very close to its current value, suggesting that \dot{E} (6.4×10^{36} erg s $^{-1}$) did not vary significantly since the supernova explosion. This state of affairs indicates that pulsar spin characteristics provide poor estimates of the ages of pulsars, and that rotating neutron stars may become pulsars with longer periods than previously thought. If this is the case, it is possible to estimate that PSR J1811–1925 was created with an initial period of ~ 62 ms (Torii et al. 1997, Kaspi et al. 2001)

The system PSR J1811–1925/G11.2-0.3 is located near the TeV source HESS J1809–193, recently discovered by the HESS telescope array (Aharonian et al. 2007). Although the pulsar is energetic enough to power the high energy gamma-rays, the association with the TeV source is not likely since the pulsar is clearly the companion of G11.2-0.3 and HESS J1809–193 is offset from the supernova remnant, implying that PSR J1811–1925 could not have produced the TeV source due to its motion. The likelihood of an association is further questioned by the presence of a second pulsar/PWN system, J1809–1917 (Kargaltsev & Pavlov 2007), which is closer to the centroid of the HESS source and also capable of supplying sufficient energy from the pulsar to power HESS J1809–193.

In this paper, we report the first observation of G11.2-0.3/PSR J1811–1925 above 10 keV by INTEGRAL/IBIS; using

the soft gamma-ray data in conjunction with archival *Chandra* observations we establish the nature of the IBIS emission and critically discuss the possibility of its association with the newly discovered HESS source.

3 THE INTEGRAL OBSERVATION

The region surrounding PSR J1811–1925 has been covered as part of the third INTEGRAL IBIS/ISGRI survey (Bird et al. 2007) processing, which consists of all exposures from the beginning of the mission (November 2002) up to April 2006. The total exposure on this region is ~ 3.5 Ms. ISGRI images for each available pointing were generated in the 18–60 keV band using the ISDC offline scientific analysis software version 5.1 (OSA 5.1; Goldwurm et al. 2003). The individual images were then combined to produce a mosaic of the entire sky to enhance the detection significance using the system described in detail by Bird et al. (2004, 2007). Figure 1 shows the image of the region surrounding PSR J1811–1925: a clear excess above the detection threshold as determined by Bird et al. (2007) is observed with a significance of $\sim 9\sigma$ at a position corresponding to R.A. = $18^{\text{h}} 11^{\text{m}} 18^{\text{s}}.35$ and Dec = $-19^{\circ} 25' 02''.64$ (J2000.0) with a positional uncertainty (90%) of $2'.9$. Within this positional uncertainty the IBIS/ISGRI excess is coincident with both SNR G11.2-0.3 and its pulsar PSR J1811–1925, despite the fact that the latter is closer to the centroid of the IBIS emission. INTEGRAL does not have sufficient angular resolution to discriminate which of these two (or other components if present) are responsible for the soft gamma-ray emission, but spectroscopic studies in conjunction with X-ray data can help to identify or eliminate the various morphological details present in the region. For this purpose, we obtained the IBIS/ISGRI spectrum following usual procedures: fluxes were extracted from the location of the source in thirteen narrow energy bands over the 17–200 keV range for all available pointings; a spectral *pha* file was then made by taking the weighted mean of the light curve obtained in each band. An appropriately re-binned *rmf* file was also produced from the standard IBIS spectral response file to match the *pha* file energy bins. The spectral analysis was performed using XSPEC v. 11.3.2; quoted errors correspond to 90% confidence levels for one interesting parameter ($\Delta\chi^2 = 2.71$).

A simple power law model provides a good fit to the IBIS/ISGRI data in the 17–200 keV energy band ($\chi^2/\text{dof} = 16.5/12$) with a photon index $\Gamma = 1.8_{-0.3}^{+0.4}$ and a 20–100 keV flux of 1.49×10^{-11} erg cm $^{-2}$ s $^{-1}$. As there is no INTEGRAL detection at the location of the TeV object, we can only derive from the IBIS/ISGRI mosaics 2σ upper limits to the flux of an undetected counterpart to be 1.7×10^{-12} and 3.1×10^{-12} erg cm $^{-2}$ s $^{-1}$ in the 20–40 and 40–100 keV energy bands respectively.

Likewise, no positive excess has been measured by INTEGRAL from the location of the nearby pulsar/PWN system PSR J1809–1917. The corresponding upper limits on the soft gamma-ray emission from this system, in the same field and with the same exposure, are similar to those given for the TeV source above, and correspond to a 2σ upper limit on the 20–100 keV luminosity of $\sim 7 \times 10^{33}$ erg s $^{-1}$ for a distance of 3.5 kpc to PSR J1809–1917. This soft γ -ray luminosity implies that PSR J1809–1917 is converting less than $\sim 0.4\%$ of its spin down power into the soft γ -ray domain.

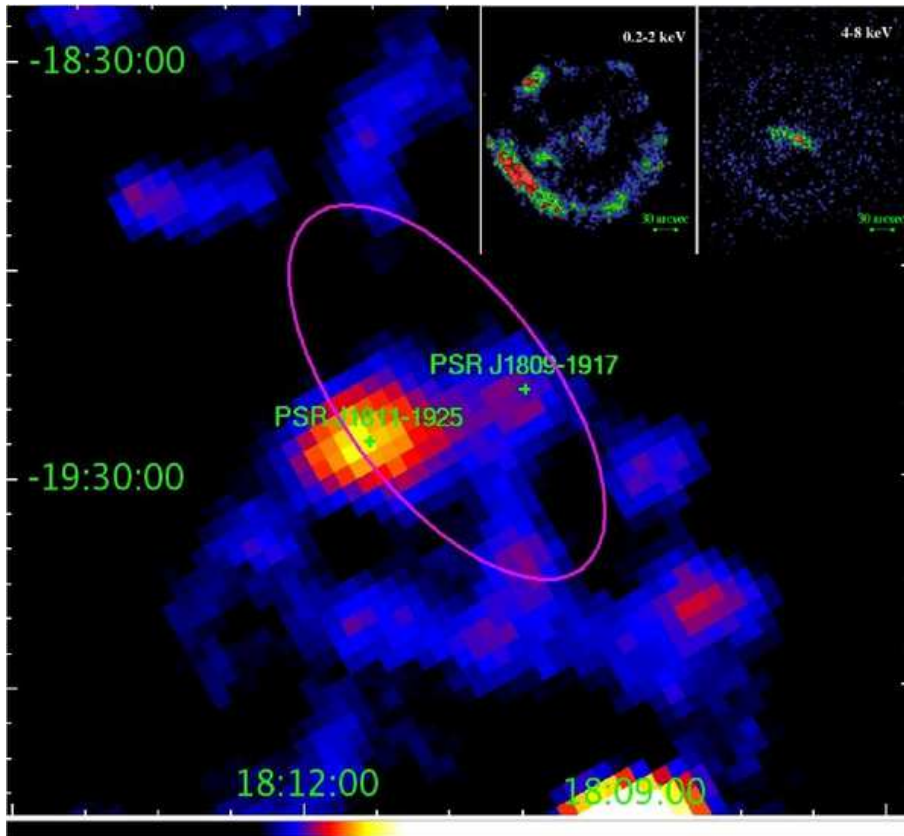


Figure 1. *INTEGRAL* IBIS/ISGRI 18–60 keV image of the region around PSR J1811–1925. Note that the image structure around the position of PSR J1809–1917 is well below the detection threshold as determined by Bird et al. (2007) for the 3rd IBIS/ISGRI catalogue. The fit ellipse (Aharonian et al. 2007) of the extended HESS source is reported with a magenta ellipse. In the inset we show the *Chandra* images ($\sim 5' \times 5'$) in 0.2–2 keV (left) and 4–8 keV (right).

4 CHANDRA OBSERVATIONS

Chandra observed the region around SNR G11.2-0.3 three times in 2000 and four times in 2003. Roberts et al. (2003) published the analysis of the observations in 2000 (20 and 15 ks), performing a spectral analysis of the different components of the system: the SNR shell, the pulsar at the centre and the elongated structure around the pulsar. This structure can be interpreted as a jet or Crab like torus seen edge-on and will be referred from now on as PSR J1811–1925 PWN. Although the X-ray images also show evidence of relativistic dynamic evolution of bright X-ray spots near the pulsar, the SNR shell, the pulsar and the PWN are the most prominent, i.e. brightest, components at these energies. With the specific aim of matching the spectral profile of these various sub-components with the *INTEGRAL* spectral emission, we reanalysed the *Chandra* observations made in 2000 and two of those performed in 2003, each having an exposure of about 15 ks. Our main goal was to gain some insight as to the location of the soft gamma-ray emission and any relevance to the HESS source. In the top inserts in Fig. 1 we show the *Chandra* images (for observation ID 3911, performed in 2000) of the region around PSR J1811–1925 in two different energy bands: 0.2–2 keV and 4–8 keV. The images clearly show that the extended PWN and the pulsar are producing the hardest X-rays while the soft (thermal) photons originate in the SNR shell. Non-thermal shell emission is also present as discussed by Roberts et al. (2003); however, this component, described by the synchrotron roll-off model, provides a null contribution if extrapolated to the IBIS energy range.

On the basis of the above considerations we can therefore exclude the SNR shell as the site of any significant emission above 10 keV.

To further investigate the spectral behaviour of the elongated region containing the jet and/or a torus, we performed a more detailed spectral analysis. We created two spectra: spectrum A was extracted from a box of $15'' \times 17''$ around the hard X-ray plume (top right inset of Fig. 1), but excluding the position of the pulsar PSR J1811–1925. Spectrum B covered the same region as spectrum A, but also included the pulsar. To avoid pile-up contamination (see Roberts et al. 2003 for details) in spectrum B we excluded the brightest central pixel in the pulsar region. For both spectra the background was taken in one circular region of $20''$ radius in the same CCD as the source. To extract spectra we used the *specextract* script of CIAO v. 3.3.0.1 for extended sources. In order to check the correctness of our procedure, we have also analysed the data not corrected for pile-up but applying a cut in energy at 5 keV as below this energy pile-up effects are not important. The fittings results obtained using both methods were the same, implying a good treatment of any pile-up problem.

To model the soft thermal emission that could still contribute to the emission in the central region near the pulsar, we employed the model proposed by Roberts et al. (2003) for both spectra A and B. This model comprises an absorbed plane-parallel shock plasma model (PSHOCK in XSPEC) with the parameters frozen to the values found in their analysis (where all regions around the SNR are fitted separately), with the exception of the absorbing column den-

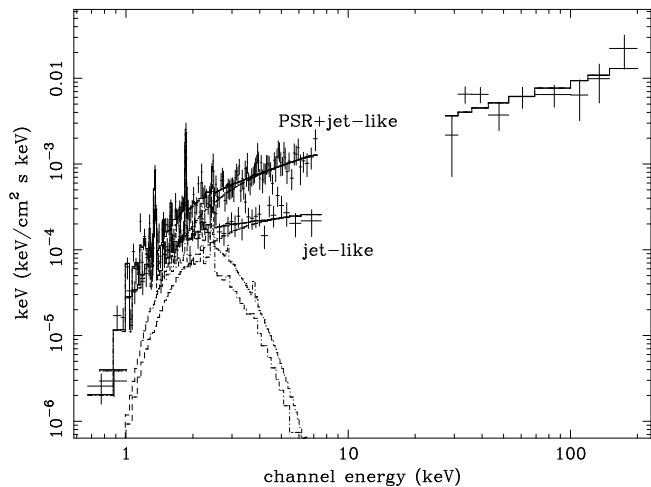


Figure 2. Composite *Chandra* and *INTEGRAL* spectra. The two data sets in the *Chandra* energy range are the spectra extracted from the jet-like feature (region A in the text) and PSR+jet-like feature (region B in the text).

sity N_{H} . We add to this component a simple power-law to fit the PWN alone or the PWN plus the pulsar. The fit we obtained is good for both spectra (A: $\chi^2/\text{dof}=48/57$, B: $\chi^2/\text{dof}=113/127$) with photon indices $\Gamma=1.7^{+0.4}_{-0.4}$ and $\Gamma=1.2^{+0.2}_{-0.2}$ for A and B respectively and $N_{\text{H}} = (2.4 \pm 0.2) \times 10^{22} \text{ cm}^{-2}$ in both spectra. The unabsorbed flux in 1–10 keV is $3.2 \times 10^{-12} \text{ erg cm}^{-2} \text{ s}^{-1}$ and $6.7 \times 10^{-12} \text{ erg cm}^{-2} \text{ s}^{-1}$ for A and B respectively. Performing similar analysis of the other *Chandra* observations made in 2003, we find completely consistent results. In Fig. 2 we show the composite *Chandra* and *INTEGRAL* spectra. In the energy range of *Chandra*, both spectra A and B are plotted. Overall our analysis is fully consistent with that of Roberts et al. (2003) both in terms of flux level and spectral shape: indeed our spectrum A has the same photon index measured by the above authors for the PWN and spectrum B is a combination of their pulsar and PWN spectra. We have also attempted to estimate a cut-off energy in the pulsar and PWN spectra. This was done by fitting spectrum B with two cut-off power-law components plus two soft PSHOCK components. All the parameters concerning the PWN were frozen to the values found fitting spectrum A, with the exception of the cut-off energy. In this way we have been able to find a lower limit to the pulsar cut-off energy at 80 keV in line with similar results found by Roberts et al. (2004) using RXTE data. Unfortunately, no information could be gained on the PWN cut-off energy.

5 ASSOCIATION WITH HESS J1809-193

Recently the HESS collaboration (Aharonian et al. 2007) have reported the detection of a new source HESS J1809–193 in this region, which they classify as a candidate PWN. HESS J1809–193 marginally overlaps with the location of PSR J1809–1917, and the centroid of the HESS emission is separated from PSR J1811–1925 by about 23 arc minutes. Kargaltsev & Pavlov (2007) have recently presented results of a *Chandra* detection of X-ray emission from the nearby pulsar J1809–1917 and have resolved its PWN. This pulsar/PWN system is situated 8' North of the HESS source centroid, but just within the HESS envelope. The pulsar is moving rapidly in the direction of the HESS source, and has an elongated PWN lying along the North-South direction, which may be explained in terms of ram pressure generated by its fast motion

through the local interstellar medium. The compact PWN appears to be inside a more extended region of X-ray emission, which is stretched towards the South of the pulsar, i.e. in the direction of HESS 1809–193. No jet, which could lie along the direction of motion and hence in the direction of the HESS source (e.g. Ng & Romani 2004), is visible in the *Chandra* images. Kargaltsev & Pavlov (2007) consider the possible but, as yet, uncertain association between PSR J1809–1917 and HESS J1809–193. Here we outline the possible, but somewhat more uncertain association between PSR J1811–1925 and HESS J1809–193.

From an energetic point of view both pulsars are capable of supplying the requisite instantaneous energy to power the HESS emission at about the 1% level of the spin down power (See Table 1). If we assume that the lifetime energy output from the pulsar is a more significant factor for determining the TeV fluxes, then for a leptonic model, we should integrate \dot{E} over the lifetime of the TeV-producing electrons, or the age of the pulsar, whichever the shorter. An electron with energy of typically 20 TeV is required to generate a 1 TeV photon by the Inverse Compton (IC) process off the Cosmic Microwave Background (CMB) and seed photons supplied from bright infrared emission from molecular clouds in the region. The associated electron lifetimes are dependent on the intensity of the ambient magnetic field as well as the rate of IC losses. During its ~ 1620 year lifetime, assuming a constant value for \dot{E} , PSR J1811–1925 is likely to release more energy than PSR J1809–1917, provided the local magnetic field is greater than $\sim 5 - 10 \mu\text{G}$. In this case the synchrotron lifetime of the TeV emitting particles is several times the age of G11.2-0.3, and therefore PSR J1809–1917 could have injected as many or more particles currently emitting at TeV energies into the surroundings than PSR J1811–1925 could have in its short lifetime.

The absence of a positive soft gamma-ray flux measurement from PSR J1809–1917 is curious. Electron energies of typically $2 \times 10^{14} \text{ eV}$ in an ambient magnetic field of $\sim 10 \mu\text{G}$ are required to create the soft γ -rays by the synchrotron process, one order of magnitude higher than those needed for the TeV photons from Compton upscatters. *INTEGRAL* observations demonstrate that PSR J1811–1925 does generate soft γ -rays and hence is visibly a better accelerator of high energy electrons. The *INTEGRAL* 20–100 keV luminosity 2σ upper limit of $\sim 7 \times 10^{33} \text{ erg s}^{-1}$ for PSR J1809–1917 implies less than 0.4% of the spin down energy is converted into soft γ -rays. If the 20–100 keV luminosity is closer to the combined PSR J1809–1917 pulsar and PWN 1–10 keV X-ray luminosity of $\sim 4.4 \times 10^{32} \text{ erg s}^{-1}$ measured by *Chandra* (Kargaltsev & Pavlov 2007), then this 20–100 keV emission will reduce to a value close to 0.05% \dot{E} . Generally the luminosities of pulsars associated with *INTEGRAL* and HESS sources share a surprisingly close fraction of the instantaneous spin down energy (e.g. Vela: *INTEGRAL* $\simeq 0.016\%$ and HESS $\simeq 0.014\%$; MSH 15-52: *INTEGRAL* $\simeq 1.8\%$ and HESS $\simeq 0.6\%$; PSR J1617–5055: *INTEGRAL* $\simeq 0.4\%$ and HESS $\simeq 1.2\%$, Carrigan et al. 2007).

An examination of the morphological details of the two pulsars and the HESS source completely reverses the situation. PSR J1809–1917 clearly provides the most plausible companion to HESS J1809–193. As the source names implies, PSR J1809–1917 is only 5 pc (taking 3.5 kpc as the distance to the pulsar) from the centroid of the VHE source, whereas PSR J1811–1925 is 29 pc away (taking a distance of 5 kpc to the pulsar). The high velocity motion of PSR J1809–1917 vectors towards the centre of the HESS source is another point in favour of an association of this pulsar to the TeV source. If the spin axis and hence possibly the putative jet are aligned with the direction of mo-

Table 1. Characteristics of the pulsars located near to the HESS J1809-193 source. L_{HESS} covers the 1–10 TeV energy range.

Pulsar	\dot{E} (erg/s)	Distance (kpc)	$L_{\text{HESS}}(\% \dot{E})$
PSR J1811–1925	6.4×10^{36}	5	0.6
PSR J1809–1917	1.8×10^{36}	3.5	1.2

tion as discussed by Ng & Romani (2004), a jet may be a possible, although unproven, mechanism to feed high energy electrons ahead of the rapidly moving pulsar and directly into the heart of HESS J1809–193. The faint X-ray structure seen in the Chandra images (Kargaltsev & Pavlov 2007) to the south of the pulsar may well provide, in future and deeper investigations, a firm observational basis for this scenario. Conversely, such evidence is lacking for PSR J1811–1925. The jet-like structure seen in the X-ray images does not point directly to the heart of the TeV source and there is no observational evidence to support the passage of energetic particles through the walls of the surrounding G11.2-0.3 supernova remnant.

6 SUMMARY & CONCLUSIONS

The INTEGRAL/IBIS telescope has detected soft γ -ray emission from the site of PSR J1811–1925. Comparison of the IBIS/ISGRI and *Chandra* spectra suggests that the soft γ -ray emission is not coming from the SNR but originates within the complex structure associated with the pulsar and its PWN system. The composite X-ray and soft γ -ray spectrum indicates the pulsar itself provides a greater fraction of the emission seen by IBIS; its spectrum is a hard power law showing no sign of a cut off up to at least 80 keV; the PWN contribution to the flux above 10 keV is smaller and well described by a steeper power law than the pulsar.

Hard (> 2 keV) pulsed X-ray emission is believed to come from the magnetosphere of the rotating neutron star and is dominated by non-thermal radiation. Two kinds of models can explain this non-thermal pulsed X/ γ -ray emission: the polar cap model (Zhang & Harding 2000) and the outer gap model (Cheng, Ho & Ruderman 1986a,b; Zhang & Cheng 1997; Wang et al. 1998; Cheng et al. 1998). In the outer gap model, the high energy emission would originate from the tail of the synchrotron component, while in the polar cap model it would stem from curvature radiation. In the latter case a spectral cut-off is expected at GeV energies while in the former a break is predicted at lower MeV frequencies. Either way, the spectral turnover is expected above the IBIS/ISGRI energy band, and broader spectral sampling is required to place constraints on any spectral break.

It is interesting to note, that a fraction of the 20–100 keV emission, roughly 50%, is coming from the PWN associated to PSR J1811–1925; i.e. this is one of the few cases (notably Crab and Vela) where emission above 10 keV is detected from a PWN. The nature of this hard X-ray emission is not yet clear, as both the synchrotron and inverse Compton processes are likely emission mechanisms. Perhaps, the Spectral Energy Distribution (SED) of INTEGRAL detected PWN could be used to tackle this issue, provided that in all cases we can separate the pulsar from the PWN as we have done here for PSR J1811–1925. Comparison with better studied objects like Crab and Vela can help in discriminating between competing models and provide more insight into the physics of PWN. To reach this objective the

close relationship between VHE gamma-ray emission and energetic young pulsars, and in a number of cases INTEGRAL sources, can be of valuable help. It is a pity that in the particular case of PSR J1811–1925 the association with HESS J1809–193 is highly improbable. PSR J1811–1925 is the most energetic young pulsar within the complex region surrounding the TeV source, but not the only one capable of providing the requisite energy. PSR J1809–1917, on balance, provides a more plausible counterpart, although it is still quite possible that neither fuels the VHE emitter, which could instead be powered by one of the supernova remnants which exist in the region.

ACKNOWLEDGEMENTS

Based on observations with INTEGRAL, an ESA project with instruments and science data centre funded by ESA member states (especially the PI countries: Denmark, France, Germany, Italy, Switzerland, Spain), Czech Republic and Poland, and with the participation of Russia and the USA. University of Southampton authors acknowledge funding from the PPARC grant PP/C000714/1. INAF/IASF–Roma and INAF/IASF–Bologna authors acknowledge funding from ASI I/R/008/07/0. The authors thank the reviewer, Mallory Roberts, for constructive criticism which has significantly improved the paper.

REFERENCES

- Aharonian, F., Akhperjanian, A.G., Bazar-Bachi, A.R. et al., 2006, *ApJ* 636, 777
- Aharonian, F., Akhperjanian, A.G., Bazar-Bachi, A.R. et al., 2007, *Astro-ph* 0705.1605
- Becker, R.H., Markert, T., & Donahue, M., 1985, *ApJ* 296, 461
- Bird, A.J., Barlow, E.J., Bassani, L., et al., 2004, *ApJ* 607, 33
- Bird, A.J., Malizia, A., Bazzano, A., et al., 2007, *ApJS* 170, 175
- Carrigan, S., Hinton, J.A., Hofman, W., Kosacki, K., Lohse, T. & Reimar, O. 2007, *astro-ph* 0709.4094
- Cheng, K.S., Ho, C., & Ruderman, M., 1986a, *ApJ* 300, 500
- Cheng, K.S., Ho, C. & Ruderman, M. 1986b, *ApJ* 300, .522
- Cheng, K. S., Gil, J., & Zhang, L. 1998, *ApJ*, 493, L35
- Gaensler, B.M., & Slane, P.O. 2006, *ARA&A* 44, 17
- Goldwurm, A., David, P., Foschini, L. et al., 2003, *A&A* 411, L223
- Green, D. A., Gull, S. F., Tan, S. M., & Simon, A. J. B., 1988, *MNRAS* 231, 73
- Helfand, D.J., Gotthelf, E.V., and Halpern, J.P., 2001, *ApJ*. 556, 380
- Kargaltsev, O. & Pavlov, G.G., 2007, *Astro-ph* 0705.2378
- Kaspi, V.M., Roberts, M.E., Vasisht, et al., 2001, *ApJ* 560, 371
- Kaspi, V.M., Roberts, M.S.E., & Harding, A.K., 2006, In *Compact Stellar X-ray Sources*, ed. W.H.G. Lewin, & M. van der Klis (Cambridge: Cambridge Univ. Press), 279
- Kirsch, M.G.F., Schonherr, G., Kendziorra, E. et al. 2006, *A&A* 453, 173
- Mangano, V., Massaro, E., Bocchino, F., Mineo, T., & Cusumano, G. 2005, *A&A* 436, 917
- Mori, H., Burrows, D.N., Hester, J.J et al, 2004, *ApJ* 609, 186
- Ng, C.-Y., & Romani, R.W., 2004, *ApJ* 601, 479
- Pavlov, G.G., Teter, M.A., Kargaltsev, O.Y. & Sanwal, D. 2003, *ApJ* 591, 115
- Roberts, M.S.E., Tam, C.R., Kaspi, V.M. et al., 2003, *ApJ* 588, 992
- Roberts, M.S.E., Ransom, S., Gavriil, F. et al., 2004, *AIP Conference Proceedings* 714, 306
- Tam, C. & Roberts, M.S.E., 2003, *ApJ* 598, 30
- Torii, K., Tsunemi, H., Dotani, T., & Mitsuda, K. 1997, *ApJ* 489, 145
- Wang, F. Y.-H., Ruderman, M., Halpern, J. P., & Zhu, T. 1998, *ApJ*, 498, 373
- Weisskopf, M.C., Wu, K., Tennant, A.F., et al. 2004, *ApJ* 605, 360

Zhang, L., & Cheng, K. S. 1997, *ApJ*, 487, 370
Zhang, B., & Harding, A. K. 2000, *ApJ*, 532, 1150